

8p

1995/08/29

324777

A REALISTIC MODEL OF EVAPORATION FOR A LIQUID DROPLET

An-Ti Chai
 NASA Lewis Research Center
 Cleveland, OH 44135

V. S. Arpaci
 Department of Mechanical Engineering
 and Applied Mechanics
 University of Michigan
 Ann Arbor, MI 48109

An intuitive delineation along with dimensional considerations and experimental evidences are presented to show that in a general case, the evaporation of a liquid droplet undergoes three regimes through the process. Initially, the heat transfer inside the evaporating droplet is conduction controlled; then, in the second stage, convective heat transfer may take over; finally, the convections subside, and the process returns to conduction controlled mode.

Consider a simple sphere of liquid droplet undergoing the evaporation process. According to the well known Maxwell's theory, the rate of evaporation can be described by the linear D-square law of quasi-steady droplet evaporation [1]:

$$-\frac{dm}{dt} = -4\pi r^2 D_{df} \frac{dc}{dr}$$

or

$$-\frac{dD^2}{dt} = 8 \frac{D_{df}}{\rho} (c_d - c_\infty)$$

where m , r , D_{df} , c , D , and ρ represent mass, radius, diffusion coefficient, concentration, droplet diameter, and liquid density, respectively. The subscript d refers to a location at the droplet surface, and subscript ∞ , a distant point or simply the ambient.

If one takes a closer look at the evaporation process, it is not difficult to realize that the classical D-square law of Maxwell does not really describe the whole process. Consider a free-floating liquid drop whose surface temperature decreases as the liquid evaporates. As the process continues, a radial

temperature gradient builds up at the free surface until the critical Marangoni number is exceeded. Then the onset of instability induces thermocapillary convective flows, which in turn speed up the evaporation. The convective flows will subside when the interior of the droplet reaches a certain equilibrium temperature, and the process will return to the conduction controlled mode.

Based on the above reasoning, the entire evaporation process can be more realistically described as follows. In the initial stage, a droplet evaporates essentially according to the D-square law and is depicted as regime I in Fig. 1. As the evaporation continues, the faster heat loss through evaporation exceeds the heat supplied through conduction and a radial temperature gradient begins to develop at the surface. Meanwhile, the Marangoni number of the droplet near the surface increases with the temperature gradient build-up. When the Marangoni number reaches its critical value, the onset of (Marangoni instability induced) convective flow commences, and this is the beginning of regime II. The convective flow effects faster heat transfer to the evaporating surface, which should result in a significant increase in the evaporation rate. Eventually, the interior temperature of the liquid drop reaches a lower (than the ambient) equilibrium value, which can not maintain the radial temperature gradient for sustaining the convective flows. At this point, the convective flow motion subsides and the process enters into the final stage of regime III. In the final stage, the liquid drop continues its evaporation at the rate sustained by the heat input from its ambient environment (excluding radiative heating), which is conduction controlled as in regime I. The process continues until the droplet evaporates completely.

While buoyancy-driven fluid problems related to spherical geometry instability have been treated to a considerable extent in the literature, the thermocapillary instability of spherical geometry has been almost completely overlooked except for the recent work of Cloot and Lebon [2] who deal with the mathematical aspects of thin spherical shell configuration, and Arpaci, Selamet, and Chai who take into consideration some physical aspects of the problem, paying special attention to realistic boundary conditions and surfactant effects [3]. To help establish the validity of the intuitive reasoning to have thermocapillary instability involved in the droplet evaporation process, the following dimensional arguments are in order.

Consider an interface momentum balance of a curved surface which is affected by the presence of surfactant

$$F_s(1-\beta) - F_v(1-R)$$

where F_s and F_v respectively denote surface tension and viscosity forces, and β and R the effect of surfactant and that of spherical curvature respectively on the cartesian Laplacian. The inertial contribution is neglected for infinitesimal instability considerations.

The thermal energy balance at the interface is

$$Q_H \sim Q_K(1+B),$$

where Q_H and Q_K respectively denote heat from enthalpy flow and conduction, and B denotes the Biot number (heat loss from the interface). Explicitly,

$$F_s \sim \Delta\sigma l, F_v \sim \mu V l, Q_H \sim \rho c_p V T l^2, Q_K \sim k T l,$$

and the equations of momentum and energy balance lead to

$$\frac{F_s(1-\beta)}{F_v(1-R)} = \frac{\Delta\sigma(1-\beta)}{\mu V(1-R)}, \quad \frac{Q_H}{Q_K(1+B)} = \frac{\rho c_p V l}{k(1+B)}$$

In the above expressions, σ , μ , ρ , c_p , and k have their conventional meanings of surface tension, viscosity, density, specific heat, and conductivity, respectively. For surface tension-driven flow, the flow velocity V is a dependent variable. Consequently, the above two expressions cannot be used as ultimate dimensionless numbers characterizing these flows. However, the combination of them in a way which eliminates the velocity V yields

$$\frac{F_s(1-\beta)}{F_v(1-R)} \frac{Q_H}{Q_K(1+B)} = \frac{1-\beta}{(1+B)(1-R)} Ma_{\beta, B, R}$$

where

$$Ma = \frac{|\Delta\sigma| l}{\mu \alpha}$$

is the usual definition of Marangoni number, l a characteristic length (liquid layer thickness), and $\alpha = k/\rho c_p$ is the thermal

diffusivity.

Now consider the case for a simple, clean and flat liquid layer. Similar arguments lead to

$$\frac{F_S Q_H}{F_V Q_K} = Ma$$

Consequently, the critical Marangoni number for a liquid droplet, relative to Ma_c for a simple, clean and flat liquid layer, can be written as

$$(Ma_{\beta, B, R})_c = \frac{(1+B)(1-R)}{1-\beta} Ma_c$$

which suggests that the heat transfer and surfactant delay, and the curvature hastens the onset of instability.

For evaporating droplets, latent heat enthalpy flow Q_2 needs to be taken into consideration in addition to the sensible heat of Q_H . Here

$$\frac{Q_H}{Q_2} \sim \frac{c_p \Delta T}{h_{fg}} = Ja$$

is the Jacob number, with h_{fg} , the latent heat. Thus for evaporating droplets, the Marangoni number needs to be replaced by

$$Ma \left(1 + \frac{1}{Ja}\right).$$

The critical Marangoni number for the onset of surface tension-driven convection in a thin layer of fluid, according to Pearson's study [4], is $Ma_c = 80$. Experiments carried out by Apollo 17 crew, however, gave an order of magnitude higher Ma_c in the range of 400 - 2,600 [5,6]. Various reasons have been cited to account for the difference, but no conclusive argument has been made.

To the best of our knowledge, similar studies for the case of an evaporating liquid droplet do not exist. The curvature is

expected to decrease the critical Marangoni number. However, a preliminary calculation has shown that the Marangoni number could reach as high as up to 10^4 for a water or methanol droplet with a radius of 1 mm, evaporating in a relatively mild (ambient temperature) environment. A Marangoni number of such a magnitude clearly indicates that the surface tension-driven convection can be expected in the evaporating droplets targeted for this study.

Ideally, accurate measurements of droplet evaporation can be performed in space using the Drop Physics Module or the Fluids Module on board the USML (United States Microgravity Laboratory), which we have already proposed to do. However, before we get the opportunity to conduct the space experiments, we are able to report here the ground-based experimental evidences (some photos were presented as poster exhibits at the VIIIth European Symposium on Materials and Fluid Sciences in Microgravity, Bruxelles, Belgium, April 13-16, 1992[7]) that unequivocally demonstrate the feasibility of conducting the experiments in space and the validity of the new model for droplet evaporation.

In order to minimize buoyancy effects and droplet deformation due to weight, we limited our sample size to approximately 1.5-1.75 mm in diameter. The sample droplet, prepared and injected at room temperature, is suspended with a wire loop inside an evaporation chamber. A sheet (approximately 0.2 mm thick) of laser light is used to illuminate a cross section of the sample; two variable intensity spot lights are used for general illumination. Flow visualization is accomplished with an Olympus microscope equipped with zoom body mechanism (7.5-64x), video and still cameras. Aluminum powder of 1 micron size is used as tracing particles. The presence of the wire loop causes a slight rotation in the bulk fluid, and the uneven heating of the loop by the illuminating light could also disturb the flow patterns. However, these undesirable effects are not as detrimental so far as our qualitative data is concerned. The flow patterns induced by thermocapillary instability can be unequivocally identified.

For evaporating liquids, we tested distilled water, methanol, acetone, and low viscosity silicon oil (Dow Corning 200 fluid, 0.65 cs). Water has been notoriously known for its suppression of surface tension-driven flows because the large dipole moment of its molecules attracts contaminations on the free surface. We certainly experienced considerable difficulty with water to induce any appreciable flows driven by surface tension forces. The volatile acetone makes it hard to obtain flow patterns steady enough for one to take photo pictures. Methanol and the 0.65 silicon oil both behave consistently well.

Figure 2(a) shows a water droplet evaporating in normal atmospheric pressure. There is no apparent internal flow of any

kind. Methanol droplets in a vapor saturated environment and a methanol droplet in the brief quasi-stationary evaporation mode (prior to the onset of instability induced convective flows) can also be represented by Fig. 2(a). Figure 2(b) shows a fairly symmetric convective flow pattern developed in an evaporating methanol (or 0.65 cs silicone oil) droplet seconds after the process gets started. However, after considerable evaporation, the temperature of the droplet decreases significantly and can no longer sustain the thermocapillary convection; the convective flows die down and the evaporation returns to conduction controlled mode. Figure 2(c) clearly shows that this is the case.

For reference and comparison, we painted a wire loop black and used it to suspend a sample droplet. Upon illumination with the sheet of laser light, the point where light intersects the loop obviously absorbed enough light to create a local warm spot, hence a surface temperature gradient on the sample droplet. The vigorous bulk flow motion exhibited in Fig. 3 was generated precisely in this manner.

REFERENCES

1. Fuchs, N. A. *Evaporation and Droplet Growth in Gaseous Media*, Pergamon Press, New York, 1959
2. Clout, A. and Lebon, G. Marangoni Convection in a Rotating Spherical Geometry, *Phys. Fluids A* 2 (4), 525-529, 1990
3. Arpaci, V. S., Selamet, E. and Chai, A. T., Thermocapillary Instability of Spherical Shells, *HTD-Vol. 180, Fundamentals of Forced and Mixed Convection and Transport Phenomena ASME* 1991
4. Pearson, J. R. A., On Convection Cells Induced by Surface Tension, *J. Fluid Mech.* 4, 489-501, 1958
5. Grodzka, P. G. and Bannister, T. C., Heat Flow and Convection Demonstration Experiments Aboard Apollo 14, *Science* 176, 506-508, 1972
6. Grodzka, P. G. and Bannister, T. C., Heat Flow and Convection Demonstration Experiments Aboard Apollo 17, *Science*, 187, 165-167, 1975
7. Chai, A. T., Rashidnia, N., and Arpaci, V. S., Marangoni Instability Induced Convection in an Evaporating Liquid Droplet, *Proceedings of the VIIth European Symposium on Materials and Fluid Sciences in Microgravity, Brussels, Belgium, 12-16 April 1992, 187-192, ESA SP-333 (August 1992)*

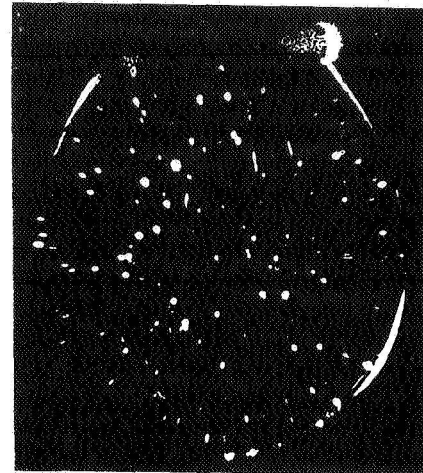
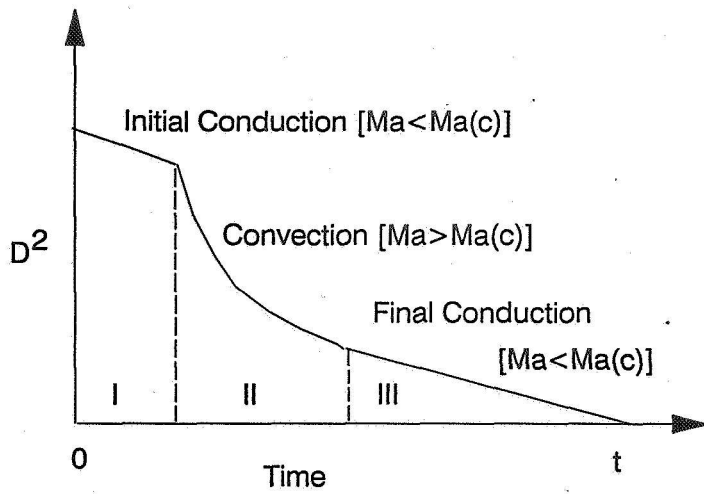


Figure 1. Three regimes of droplet evaporation

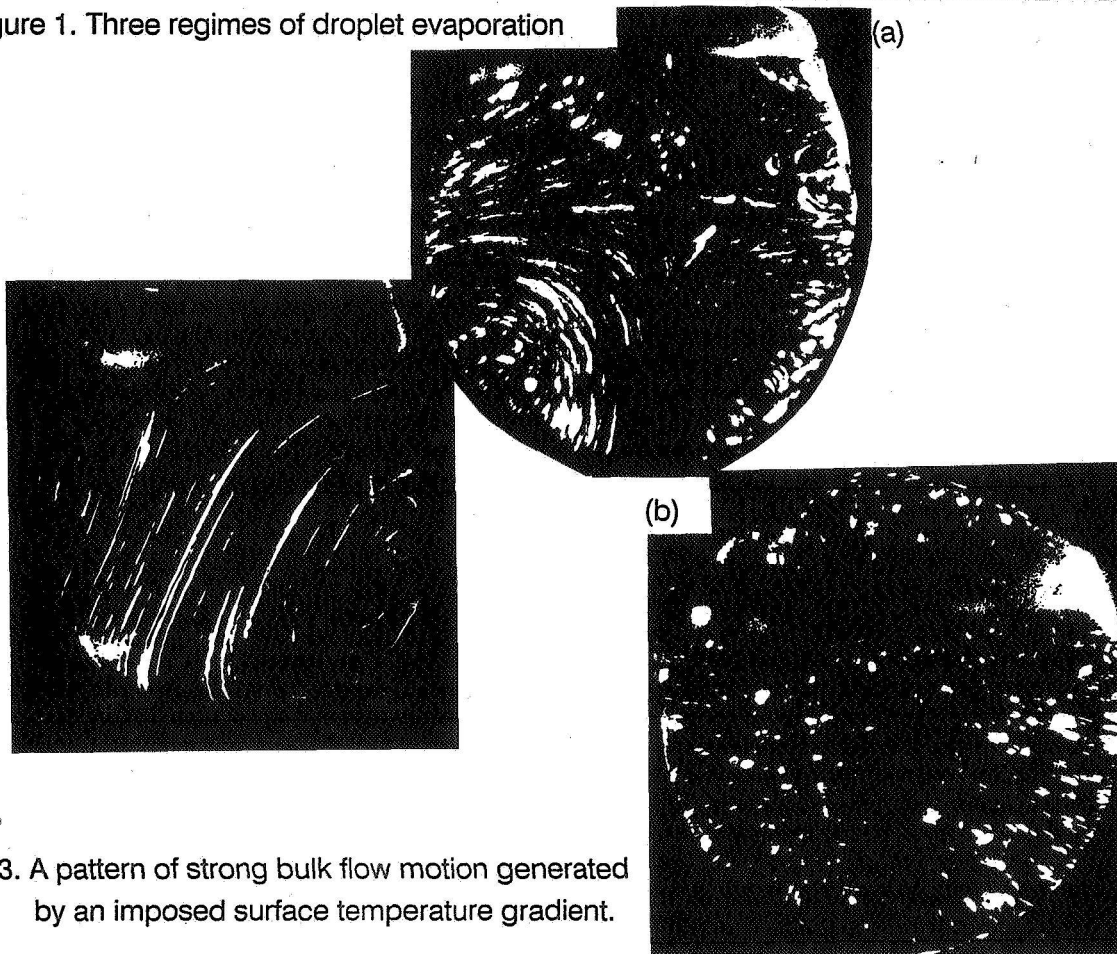


Figure 3. A pattern of strong bulk flow motion generated by an imposed surface temperature gradient.

Figure 2. Laser sheet light illuminated cross section of an evaporating droplet (a) in regime I (b) in regime II, (c) in regime III.